JACS
JOURNAL OF THE AMERICAN CHEMICAL SOCIETY
Communication
pubs.acs.org/JACS

How Cinchona Alkaloid-Derived Primary Amines Control Asymmetric Electrophilic Fluorination of Cyclic Ketones

Yu-hong Lam and K. N. Houk*

Department of Chemistry and Biochemistry, University of California, Los Angeles, 607 Charles E. Young Drive East, Los Angeles, California 90095-1569, United States

Supporting Information

ABSTRACT: The origin of selectivity in the α-fluorination of cyclic ketones catalyzed by cinchona alkaloid-derived primary amines is determined with density functional calculations. The chair preference of a seven-membered ring at the fluorine transfer transition state is key in determining the sense and level of enantiofacial selectivity.

Asymmetric fluorination[1] is important in organic synthesis due to the unique properties of fluorine[2] that have proven of value in the pharmaceutical and material sciences.[3] Cinchona alkaloids have been prominently featured from the infancy of asymmetric fluorination.[4] The quinidine-derived primary amine **I**[5] and a related cinchonine were identified by MacMillan,[6] using high-throughput screening, as highly selective catalysts for the α-monofluorination of a wide variety of cyclic ketones (**1**−**5**) with *N*-fluorobenzenesulfonimide (NFSI) (Scheme 1).[7] This represents significant progress toward the solution of the so-called "ketone fluorination problem," since pyrrolidine- and imidazolidinone-based organocatalysts, while successful in the catalytic fluorination of aldehydes,[8] fail to give high yields or enantioselectivities with ketones.[6,8e] No rationale of the origin of stereocontrol has been proposed, although MacMillan suggested that the reactions may proceed by dual activation of the ketone and the fluorine source.[6]

Scheme 1. MacMillan's Fluorination of Cyclic Ketones Organocatalyzed by Cinchona Alkaloid−Primary Amines

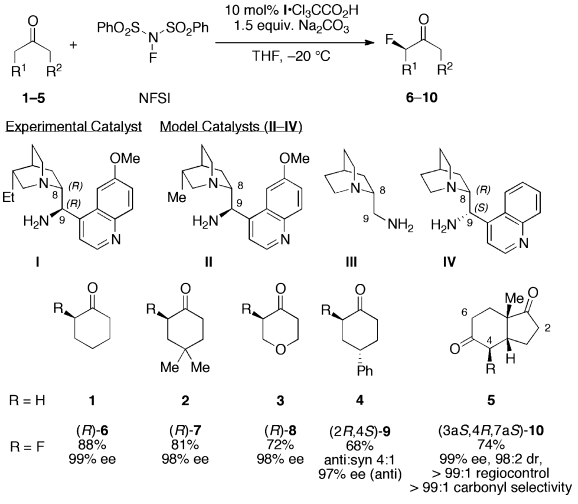

The understanding of the structural basis of asymmetric induction by cinchona alkaloids and their derivatives in organocatalysis has been remarkably underdeveloped,[9] although some progress has been made recently.[10] The origins of stereocontrol in any enamine-activated transformations catalyzed by cinchona alkaloid−primary amines, however, have not been studied. We now present quantum chemical computations for MacMillan's asymmetric fluorination catalyzed by **I**. We explain how the cinchona alkaloid scaffold achieves high levels of enantiofacial control by adopting well-defined conformations at the cyclic fluorine transfer transition state.

Geometry optimizations and frequency computations were performed using *Gaussian 09*[11] at the B3LYP/6-31G(d) level of theory[12] in conjunction with the IEF-PCM model[13] to account for the solvation effects of tetrahydrofuran, the solvent used experimentally. Single-point energies of the fluorination transition structures were also calculated using B3LYP-D3(BJ),[14] M06-2X,[15] and ωB97XD[16] functionals with the def2-TZVPP[17] basis set.[18] B3LYP-D3(BJ)/def2-TZVPP-IEF-PCM//B3LYP/6-31G(d)-IEF-PCM results are presented in the main text, but all the other density functional methods tested yield identical trends and similar magnitudes in the relative free energies of activation ($\Delta\Delta G^{\ddagger}$) of the stereoisomeric TSs. Thus, the same conclusions about the structural origins of selectivity are reached irrespective of the functional used.[18]

MacMillan reported that NFSI was premixed with the organocatalyst, before the ketone was added.[6] Fluorine transfer to the quinuclidine nitrogen of cinchona alkaloids from several electrophilic fluorinating reagents, including NFSI, is well-known[19] and forms the basis of asymmetric fluorination promoted stoichiometrically or catalytically by cinchona alkaloid derivatives.[20] At the CBS-QB3 level of theory, starting from the enamine derived from acetone and ammonia, the free energy of activation ($\Delta G^{\ddagger}$) for the bimolecular fluorine transfer is 6.6 kcal/mol from the *N*-fluorotrimethylammonium ion (Me_3NF^+) and 21.3 kcal/mol from *N*-fluoromethanesulfonimide ($(MeSO_2)_2NF$).[18] Density functional methods including B3LYP, B3LYP-D3(BJ), M06-2X, and ωB97XD predict similarly large differences in reactivity.[18,21] It is also experimentally known that *N*-fluoroquinuclidinium salts are a stronger fluorinating reagent than NFSI.[22] Thus, the C−F bonds in products **6**−**10** are predicted to be formed from the enamine predominantly via

Received: May 12, 2014
Published: June 26, 2014

   dx.doi.org/10.1021/ja504714m | J. Am. Chem. Soc. 2014, 136, 9556−9559

intramolecular attack on the quinuclidine nitrogen-bound fluorine, rather than an intermolecular reaction with NFSI.

We computed the TSs for the intramolecular N-to-C fluorine transfer to either face of the enamine formed from **1** and model catalyst **II** (**TS-6a**–**6b**, Figure 1). The free energy of activation

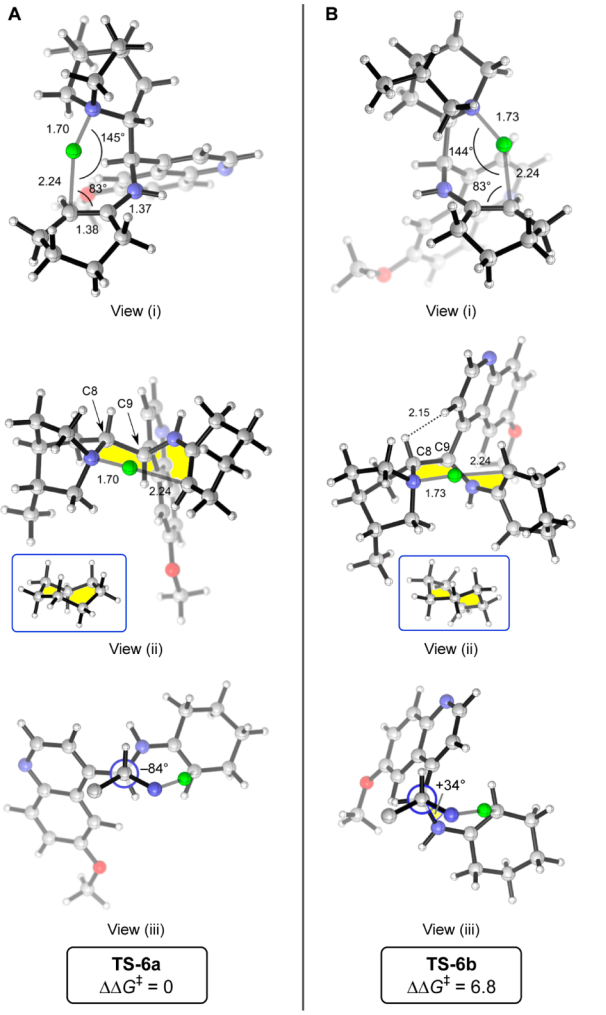

Figure 1. Stereochemistry-determining transition structures **TS-6a** (A) and **TS-6b** (B) for fluorination of **1** (B3LYP-D3(BJ)/def2-TZVPP-IEF-PCM (THF)//B3LYP/6-31G(d)-IEF-PCM (THF)), each shown in three views. In view (ii), the fluorine transfer ring is color-filled and compared to its analogous cycloheptane conformer in the blue inset (ref 24). View (iii) shows the Newman projection along the C8–C9 bond, omitting the quinuclidine moiety for clarity. The difference in free energy of activation ($\Delta\Delta G^{\ddagger}$) is reported, relative to **TS-6a**, in kcal/mol.

($\Delta G^{\ddagger}$) for this step is 8.6 kcal/mol. The formation of (*R*)-**6** via **TS-6a** is favored over the formation of (*S*)-**6** via **TS-6b** by 6.8 kcal/mol, in agreement with the very high enantioselectivity reported (99% ee).[23]

Salient features of **TS-6a** and **TS-6b** are illustrated from three views in Figure 1. The first view shows that the fluorination proceeds by axial attack of fluorine on the half-chair cyclohexene ring; the equatorial attack TSs, **TS-6c** and **TS-6d**,[18] are less stable by 1.1 kcal/mol than **TS-6a** and **TS-6b**, respectively. **TS-6a** and **TS-6b** have practically the same N–F and F–C partial bond distances as well as N–F–C and F–C–C angles. The key difference between these TSs lies in their conformation, as revealed by view (ii) in Figure 1. The seven-membered fluorine transfer rings in **TS-6a** and **TS-6b** have conformations that are closely comparable to the well-established conformations of cycloheptane (blue inset, Figure 1)[24] and control the facial selectivity of the enamine. In **TS-6a**, this ring adopts a chair conformation, exposing the C*α-Re* face to attack by fluorine, whereas **TS-6b** adopts a boat conformation and the opposite enantioface is accessible. The third perspective focuses on the conformation about the C8–C9 bond. In **TS-6a**, the N–C8 and C9–N bonds are almost orthogonal, presumably alleviating electrostatic repulsion between the nitrogens, while the boat-type conformation of **TS-6b** brings the two C–N bonds closer together at a dihedral angle of 34°, resulting in higher eclipsing strain.

An interesting feature concerning facial control is that, in both **TS-6a** and **TS-6b**, the starting enamine is s-cis about the N–C bond. In other words, the two enantiofaces of the enamine are distinguished not by the conformation about the enamine N–C bond, as is well established with pyrrolidine and imidazolidinone-based organocatalysts,[25] but by the conformation about the C8–C9 bond of the cinchona amine instead.

The level of chair preference of the ring was assessed by computing the fluorination TSs **TS-11a** and **TS-11b**, derived from **1** and model catalyst **III**, devoid of the quinoline ring on C9 (as well as the methyl group on the cage) (Figure 2). The *R*

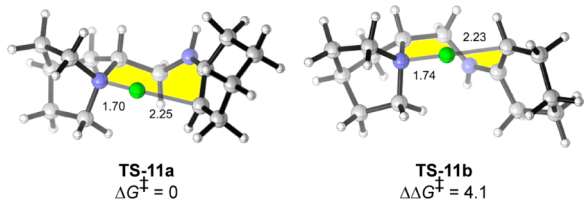

Figure 2. Transition structures **TS-11a** and **TS-11b** derived from **1** and model catalyst **III** (B3LYP-D3(BJ)/def2-TZVPP-IEF-PCM (THF)//B3LYP/6-31G(d)-IEF-PCM (THF)). The difference in free energy of activation ($\Delta\Delta G^{\ddagger}$) is reported, relative to **TS-11a**, in kcal/mol.

enantiomer is still predicted to be favored, but to a lesser extent ($\Delta\Delta G^{\ddagger}$ = 4.1 kcal/mol). The presence of an *R*-configured quinoline substituent on C9 of **II** widens the energy difference between the stereoisomeric TSs, because **TS-6a** places the quinoline ring at an equatorial site of the chair ring; in **TS-6b**, the quinoline is axial and comes into steric contact with the hydrogen on C8. *Thus, the high facial selectivity of fluorination stems from two factors: (1) the preferred conformation of the seven-membered ring, and (2) the steric bulk of the C9-quinoline of the organocatalyst.* Catalysts **I** and **II** possess *like* relative configurations at C8 and C9 (both chirality centers are *R*). This places, in **TS-6a**, the C9-bulky group in a more favorable equatorial position of a lower-energy chairlike ring. *In other words, the two factors are matched and conducive to fluorine transfer via a low-energy transition state.*

It follows from this analysis that inverting the configuration of C9 will cause the fluorine transfer to be less favorable, since the two factors are now mismatched. To ascertain the impact of this mismatch, computations were performed on the fluorination transition structures **TS-12a** and **TS-12b** derived from **1** and model catalyst **IV**, which features *unlike* configurations at C8 and C9 (Figure 3). The chair **TS-12a** is now higher in energy than **TS-12b** by 7.6 kcal/mol, indicating that an axial substituent destabilizes the fluorine transfer TS more than a boat conformation. The fluorine transfer is predicted to be more difficult: the free energy of activation is 2.0 kcal/mol higher than in the case of **TS-6a**. This is qualitatively in line with the

dx.doi.org/10.1021/ja504714m | *J. Am. Chem. Soc.* 2014, 136, 9556–9559

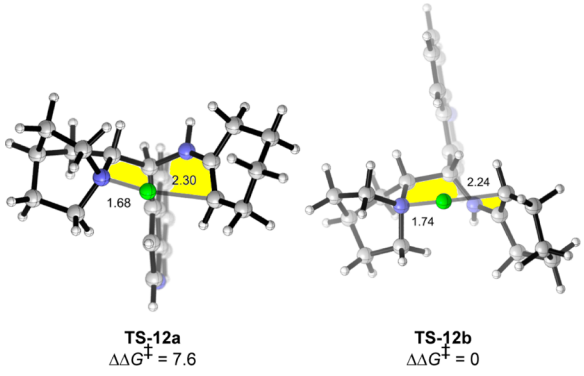

Figure 3. Transition structures **TS-12a** and **TS-12b** derived from **1** and model catalyst **IV** (B3LYP-D3(BJ)/def2-TZVPP-IEF-PCM (THF)//B3LYP/6-31G(d)-IEF-PCM (THF)). The difference in free energy of activation ($\Delta\Delta G^{\ddagger}$) is reported, relative to **TS-12b**, in kcal/mol.

observation[7] that a pseudoenantiomer of **IV** gives poor conversion in the fluorination of the piperidinone ring.

The sense and level of enantioselectivities observed with the fluorination of other cyclic ketones reported (Scheme 1) are also consistent with this model. The fluorinations of **2** and **3** are predicted to favor the *R* enantiomer by 7.2 and 7.1 kcal/mol, respectively.[18] The desymmetrizing fluorination of **4** occurs with an anti/syn selectivity of 4:1, with the major product, (2*R*,4*S*)-**9**, formed in 97% ee. As shown in Figure 4, the energy difference between the (2*R*,4*S*) transition state **TS-9a** and the (2*S*,4*R*) transition state **TS-9b** is 7.1 kcal/mol, consistent with the high enantioselectivity observed for the anti diastereomer. The energy

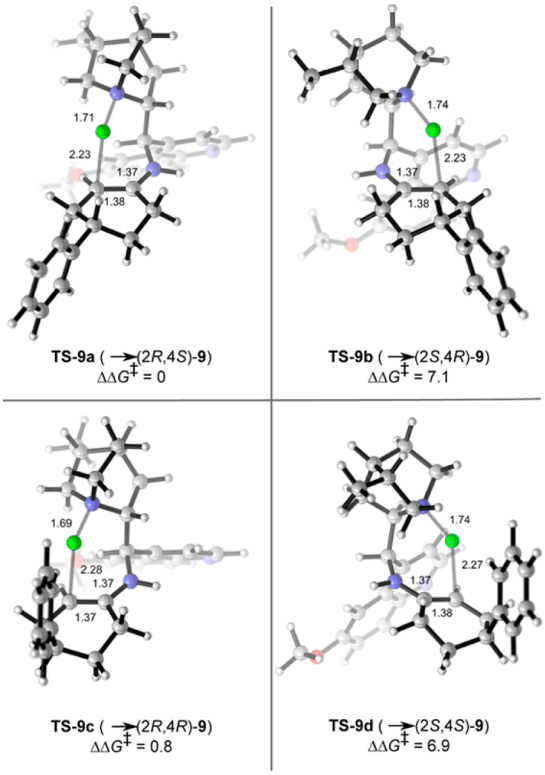

Figure 4. Lowest-energy stereoisomeric transition structures **TS-9a−d** for fluorination of **4** (B3LYP-D3(BJ)/def2-TZVPP-IEF-PCM (THF)//B3LYP/6-31G(d)-IEF-PCM (THF)). The differences in free energy of activation ($\Delta\Delta G^{\ddagger}$) are reported, relative to **TS-9a**, in kcal/mol.

difference of 0.8 kcal/mol between **TS-9a** and the (2*R*,4*R*) transition state **TS-9c** also agrees well with the moderate diastereoselectivity experimentally found.

The model can be extended to more elaborate substrate structures. The fluorination of bicyclic diketone **5** catalyzed by **I** affords the C4-monofluorinated product (3a*S*,4*R*,7a*S*)-**10** in 74% yield and 98:2 dr (4*R* vs 4*S*) (Scheme 1). The regioisomeric fluorination transition structures **TS-10a−c** featuring a chairlike seven-membered ring are shown in Figure 5. The major product

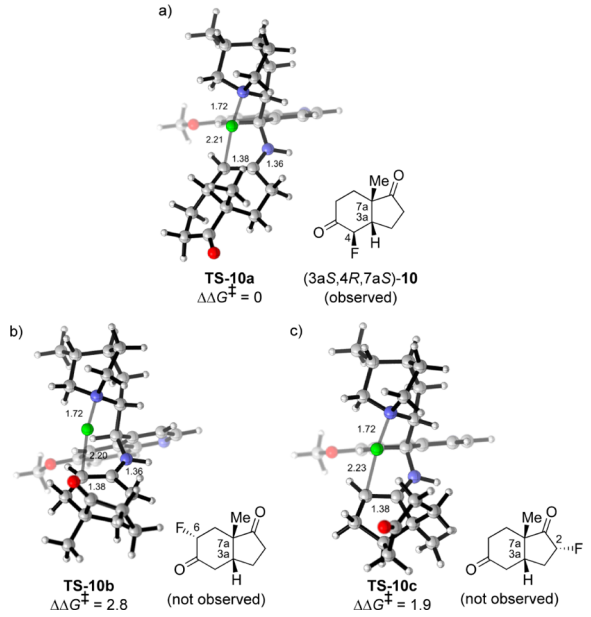

Figure 5. Transition structures **TS-10a−c** for fluorination of **5** (B3LYP-D3(BJ)/def2-TZVPP-IEF-PCM (THF)//B3LYP/6-31G(d)-IEF-PCM (THF)). Only the chairlike transition structures are illustrated. The differences in free energy of activation ($\Delta\Delta G^{\ddagger}$) are reported, relative to **TS-10a**, in kcal/mol.

originates from an enamine that is nucleophilic at C4. Indeed, **TS-10a**, which models fluorine transfer to C4, is the most favored; **TS-10b** and **TS-10c**, which model fluorine transfer to the two other α-positions of **5**, are, respectively, 2.8 and 1.9 kcal/mol higher in free energy and thus have negligible contributions to the formation of the alternative fluorinated regioisomers.

In summary, we have proposed the first stereoselectivity model for an enamine-activated cinchona amine-catalyzed reaction (see Table of Contents graphic). For the fluorinations of cyclic ketones catalyzed by **I**, the major enantiomer arises from a seven-membered fluorine transfer cyclic TS in a chair conformation. Enantiofacial discrimination is achieved by control of the conformation of this ring. The effectiveness of catalyst **I** is in line with the equatorial preference of its C9-substituent at the fluorine transfer TS. Work is in progress to apply this novel stereocontrolling proposal to explain and predict other cinchona alkaloid−primary amine catalyzed α-functionalization reactions.[26]

■ ASSOCIATED CONTENT

Ⓢ Supporting Information

Fluorination TSs involving *N*-fluorotrimethylammonium ion and *N*-fluoromethanesulfonimide. Complete set of TSs for fluorination of **1** (**TS-6a−6d**). Illustrations of geometries of TSs for fluorination of **2** and **3**. Computational results by other density functionals. Cartesian coordinates and thermodynamic

dx.doi.org/10.1021/ja504714m | J. Am. Chem. Soc. 2014, 136, 9556−9559

parameters (in hartrees) of all stationary points. This material is available free of charge via the Internet at http://pubs.acs.org.

AUTHOR INFORMATION

Corresponding Author

houk@chem.ucla.edu

Notes

The authors declare no competing financial interest.

ACKNOWLEDGMENTS

Financial support is provided by the National Institute of General Medical Sciences, National Institutes of Health (GM36700). The computational resources from the UCLA Institute for Digital Research and Education, and from the National Science Foundation through XSEDE resources provided by the XSEDE Science Gateways program are gratefully acknowledged.

REFERENCES

(1) (a) Liang, T.; Neumann, C. N.; Ritter, T. *Angew. Chem., Int. Ed.* **2013**, *52*, 8214. (b) Cahard, D.; Xu, X.; Couve-Bonnaire, S.; Pannecoucke, X. *Chem. Soc. Rev.* **2010**, *39*, 558. (c) Valero, G.; Companyó, X.; Rios, R. *Chem.—Eur. J.* **2011**, *17*, 2018.

(2) (a) Cahard, D.; Bizet, V. *Chem. Soc. Rev.* **2014**, *43*, 135. (b) O'Hagan, D. *J. Org. Chem.* **2012**, *77*, 3689. (c) Zimmer, L. E.; Sparr, C.; Gilmour, R. *Angew. Chem., Int. Ed.* **2011**, *50*, 11860.

(3) (a) Ojima, I. *J. Org. Chem.* **2013**, *78*, 6358. (b) Purser, S.; Moore, P. R.; Swallow, S.; Gouverneur, V. *Chem. Soc. Rev.* **2008**, *37*, 320. (c) Muller, K.; Faeh, F.; Diederich, F. *Science* **2007**, *317*, 1881. (d) Bremer, M.; Kirsch, P.; Klasen-Memmer, M.; Tarumi, K. *Angew. Chem., Int. Ed.* **2013**, *52*, 8880.

(4) (a) Shibata, N.; Suzuki, E.; Takeuchi, Y. *J. Am. Chem. Soc.* **2000**, *122*, 10728. (b) Cahard, D.; Audouard, C.; Plaquevent, J.-C.; Roques, N. *Org. Lett.* **2000**, *2*, 3699.

(5) (a) Brunner, H.; Bügler, J.; Nuber, B. *Tetrahedron: Asymmetry* **1995**, *6*, 1699. (b) Cassani, C.; Martín-Rapún, R.; Arceo, E.; Bravo, F.; Melchiorre, P. *Nat. Protoc.* **2013**, *8*, 325.

(6) Kwiatkowski, P.; Beeson, T. D.; Conrad, J. C.; MacMillan, D. W. C. *J. Am. Chem. Soc.* **2011**, *133*, 1738.

(7) Shaw, S. J.; Goff, D. A.; Boralsky, L. A.; Irving, M.; Singh, R. *J. Org. Chem.* **2013**, *78*, 8892.

(8) (a) Dinér, P.; Kjærsgaard, A.; Lie, M. A.; Jørgensen, K. A. *Chem.—Eur. J.* **2008**, *14*, 122. (b) Marigo, M.; Fielenbach, D.; Braunton, A.; Kjærsgaard, A.; Jørgensen, K. A. *Angew. Chem., Int. Ed.* **2005**, *44*, 3703. (c) Steiner, D. D.; Mase, N.; Barbas, C. F., III. *Angew. Chem., Int. Ed.* **2005**, *44*, 3706. (d) Beeson, T. D.; MacMillan, D. W. C. *J. Am. Chem. Soc.* **2005**, *127*, 8826. (e) Enders, D.; Hüttl, M. R. M. *Synlett* **2005**, 991.

(9) (a) Duan, J.; Li, P. *Catal. Sci. Technol.* **2014**, *4*, 311. (b) Melchiorre, P. *Angew. Chem., Int. Ed.* **2012**, *51*, 9748. (c) Jiang, L.; Chen, Y.-C. *Catal. Sci. Technol.* **2011**, *1*, 354. (d) Marcelli, T.; Hiemstra, H. *Synthesis* **2010**, 1229. (e) Connon, S. J. *Chem. Commun.* **2008**, 2499.

(10) Recent reports: (a) Xue, X.-S.; Li, X.; Yu, A.; Yang, C.; Song, C.; Cheng, J.-P. *J. Am. Chem. Soc.* **2013**, *135*, 7462. (b) Lifchits, O.; Mahlau, M.; Reisinger, C. M.; Lee, A.; Farès, C.; Polyak, I.; Gopakumar, G.; Thiel, W.; List, B. *J. Am. Chem. Soc.* **2013**, *135*, 6677. (c) Moran, A.; Hamilton, A.; Bo, C.; Melchiorre, P. *J. Am. Chem. Soc.* **2013**, *135*, 9091. (d) Yang, H.; Wong, M. W. *J. Am. Chem. Soc.* **2013**, *135*, 5808. (e) Zhu, J.-L.; Zhang, Y.; Liu, C.; Zheng, A.-M.; Wang, W. *J. Org. Chem.* **2012**, *77*, 9813. (f) Sengupta, A.; Sunoj, R. B. *J. Org. Chem.* **2012**, *77*, 10525. (g) Cucinotta, C. S.; Kosa, M.; Melchiorre, P.; Cavalli, A.; Gervasio, F. L. *Chem.—Eur. J.* **2009**, *15*, 7913. Reviews: (h) Marcelli, T. *WIREs Comput. Mol. Sci.* **2011**, *1*, 142. (i) Cheong, P. H.-Y.; Legault, C. Y.; Um, J. M.; Çelebi-Ölçüm, N.; Houk, K. N. *Chem. Rev.* **2011**, *111*, 5042.

(11) Frisch, M. J.; Trucks, G. W.; Schlegel, H. B.; Scuseria, G. E.; Robb, M. A.; Cheeseman, J. R.; Scalmani, G.; Barone, V.; Mennucci, B.; Petersson, G. A.; Nakatsuji, H.; Caricato, M.; Li, X.; Hratchian, H. P.; Izmaylov, A. F.; Bloino, J.; Zheng, G.; Sonnenberg, J. L.; Hada, M.; Ehara, M.; Toyota, K.; Fukuda, R.; Hasegawa, J.; Ishida, M.; Nakajima, T.; Honda, Y.; Kitao, O.; Nakai, H.; Vreven, T.; Montgomery, J. A., Jr.; Peralta, J. E.; Ogliaro, F.; Bearpark, M.; Heyd, J. J.; Brothers, E.; Kudin, K. N.; Staroverov, V. N.; Keith, T.; Kobayashi, R.; Normand, J.; Raghavachari, K.; Rendell, A.; Burant, J. C.; Iyengar, S. S.; Tomasi, J.; Cossi, M.; Rega, N.; Millam, J. M.; Klene, M.; Knox, J. E.; Cross, J. B.; Bakken, V.; Adamo, C.; Jaramillo, J.; Gomperts, R.; Stratmann, R. E.; Yazyev, O.; Austin, A. J.; Cammi, R.; Pomelli, C.; Ochterski, J. W.; Martin, R. L.; Morokuma, K.; Zakrzewski, V. G.; Voth, G. A.; Salvador, P.; Dannenberg, J. J.; Dapprich, S.; Daniels, A. D.; Farkas, O.; Foresman, J. B.; Ortiz, J. V.; Cioslowski, J.; Fox, D. J. *Gaussian 09*, Rev. D.01; Gaussian, Inc.: Wallingford, CT, 2013.

(12) (a) Becke, A. D. *J. Chem. Phys.* **1993**, *98*, 5648. (b) Lee, C.; Yang, W.; Parr, R. G. *Phys. Rev. B* **1988**, *37*, 785. (c) Vosko, S. H.; Wilk, L.; Nusair, M. *Can. J. Phys.* **1980**, *58*, 1200. (d) Stephens, P. J.; Devlin, F. J.; Chabalowski, C. F.; Frisch, M. J. *J. Phys. Chem.* **1994**, *98*, 11623.

(13) Tomasi, J.; Mennucci, B.; Cammi, R. *Chem. Rev.* **2005**, *105*, 2999.

(14) (a) Grimme, S.; Antony, J.; Ehrlich, S.; Krieg, H. *J. Chem. Phys.* **2010**, *132*, 154104. (b) Grimme, S.; Ehrlich, S.; Goerigk, L. *J. Comput. Chem.* **2011**, *32*, 1456. (c) Johnson, E. R.; Becke, A. D. *J. Chem. Phys.* **2006**, *124*, 174104. (d) Johnson, E. R.; Becke, A. D. *J. Chem. Phys.* **2005**, *123*, 024101.

(15) Zhao, Y.; Truhlar, D. *Theor. Chem. Acc.* **2008**, *120*, 215.

(16) Chai, J.-D.; Head-Gordon, M. *Phys. Chem. Chem. Phys.* **2008**, *10*, 6615.

(17) Weigend, F.; Ahlrichs, R. *Phys. Chem. Chem. Phys.* **2005**, *7*, 3297.

(18) See Supporting Information (SI) for details.

(19) Baudequin, C.; Loubassou, J.-F.; Plaquevent, J.-C.; Cahard, D. *J. Fluorine Chem.* **2003**, *122*, 189.

(20) (a) Ishimaru, T.; Shibata, N.; Horikawa, T.; Yasuda, N.; Nakamura, S.; Toru, T.; Shiro, M. *Angew. Chem., Int. Ed.* **2008**, *47*, 4157. (b) Greedy, B.; Paris, J.-M.; Vidal, T.; Gouverneur, V. *Angew. Chem., Int. Ed.* **2003**, *42*, 3291. (c) Tanzer, E.-M.; Schweizer, W. B.; Ebert, M.-O.; Gilmour, R. *Chem.—Eur. J.* **2012**, *18*, 2006. See also ref 4.

(21) The UB3LYP/6-31G(d) wave function optimized for the TS for fluorine transfer from Me_3NF^+ is identical to the RB3LYP/6-31G(d) wave function, confirming that spin-restricted DFT calculations are appropriate for modeling the fluorine transfers in our work. See SI for details.

(22) Gilicinski, A. G.; Pez, G. P.; Syvret, R. G.; Lal, G. S. *J. Fluorine Chem.* **1992**, *59*, 157.

(23) For **TS-6a** and **TS-6b**, the $\Delta\Delta G^{\ddagger}$ values calculated using B3LYP-D3(BJ)/def2-TZVPP−IEF-PCM single-point energies and *fully optimized* B3LYP-D3(BJ)/TZVP-IEF-PCM geometries and thermal corrections are 0 and 6.5 kcal/mol, respectively. This confirms that B3LYP/6-31G(d) yields adequate TS geometries to be used in energy calculations with a dispersion-inclusive functional and a larger basis set. See also: Simón, L.; Goodman, J. M. *Org. Biomol. Chem.* **2011**, *9*, 689.

(24) Wiberg, K. B. *J. Org. Chem.* **2003**, *68*, 9322.

(25) Allemann, C.; Gordillo, R.; Clemente, F. R.; Cheong, P. H.-Y.; Houk, K. N. *Acc. Chem. Res.* **2004**, *37*, 558.

(26) (a) Lifchits, O.; Demoulin, N.; List, B. *Angew. Chem., Int. Ed.* **2011**, *50*, 9680. (b) Jadhav, M. S.; Righi, P.; Marcantoni, E.; Bencivenni, G. *J. Org. Chem.* **2012**, *77*, 2667.